

# Development of Tensile Stress-Strain Relationship for High-Strength Steel Fiber Reinforced Concrete

H. A. Alguhi, W. A. Elsaigh

**Abstract**—This paper provides a tensile stress-strain ( $\sigma$ - $\epsilon$ ) relationship for High-Strength Steel Fiber Reinforced Concrete (HSFRC). Load-deflection ( $P$ - $\delta$ ) behavior of HSFRC beams tested under four-point flexural load were used with inverse analysis to calculate the tensile  $\sigma$ - $\epsilon$  relationship for various tested concrete grades (70 and 90MPa) containing 60 kg/m<sup>3</sup> (0.76 %) of hook-end steel fibers. A first estimate of the tensile ( $\sigma$ - $\epsilon$ ) relationship is obtained using RILEM TC 162-TDF and other methods available in literature, frequently used for determining tensile  $\sigma$ - $\epsilon$  relationship of Normal-Strength Concrete (NSC) Non-Linear Finite Element Analysis (NLFEA) package ABAQUS<sup>®</sup> is used to model the beam's  $P$ - $\delta$  behavior. The results have shown that an element-size dependent tensile  $\sigma$ - $\epsilon$  relationship for HSFRC can be successfully generated and adopted for further analyses involving HSFRC structures.

**Keywords**—Tensile stress-strain, flexural response, high strength concrete, steel fibers, non-linear finite element analysis.

## I. INTRODUCTION

CONCRETE is known to be brittle material with low tensile strength, a propriety often neglected when designing conventionally reinforced concrete structures. However, some structures such as; concrete ground slabs are mainly designed relying on flexural capacity of concrete. In recent years, the flexural capacity of Normal-Strength Concrete (NSC) ground slabs has been improved by adding steel fiber to concrete. Adding steel fibers to concrete is found to delay crack opening, thus improves ductility and toughness of the ground slabs [1]. The benefits of High-Strength Concrete (HSC) are widely recognized and eventually used in many reinforced concrete structures. In contrast the material use in ground slabs application is either not exist or rare. This may attribute to the relatively higher brittleness of HSC as compared to NCS, which is expected to induce more corner and edge cracks as far as ground slabs are considered. Considerable literature indicates that addition of steel fibers to HSC alters its brittleness to a more ductile material, making it suitable for ground slab.

Finite element analysis of HSFRC ground slabs requires an appropriate constitutive model describing the tensile stress-strain ( $\sigma$ - $\epsilon$ ) relationship of the material. Several techniques have been proposed to determine the tensile  $\sigma$ - $\epsilon$  relationship of NSC with steel fiber containing various a mounts of steel fibers. RILEM TC 162-TDF [2], developed the tensile ( $\sigma$ - $\epsilon$ ) relationship, based on the fracture energy, which utilizes results from a deformation-controlled beam-bending test. Moreover,

[3], proposed some modifications to the original RILEM method. It is worth pointing that both models consider NSC with containing relatively low amounts of steel fibers (10-45 kg/m<sup>3</sup>). A more general approach is the inverse analysis, which is becoming more attractive and gaining the attention of research in the past few years [4]–[8]. The inverse analysis basically uses an experimental flexural response, generated from four-point bending beam test, to back calculate the tensile  $\sigma$ - $\epsilon$  relationship of the beam's material. The advantage of this approach is that it can estimate the complexities regarding direct tensile test and fiber-matrix interaction. It is worth nothing that concrete grade and steel fiber parameters will both have significant effect on the tensile  $\sigma$ - $\epsilon$  relationship.

This paper is part of a research project conducted at King Saud University, looking in to potential use of HSFRC in ground slab applications. The aim is to develop tensile  $\sigma$ - $\epsilon$  relationship for HSFRC, which can be used in Non-Linear Finite Element Analysis (NLFEA) of ground slabs. The objectives of this paper are:

- Evaluation of tensile  $\sigma$ - $\epsilon$  relationship developed using the existing approaches.
- Generate tensile  $\sigma$ - $\epsilon$  relationship using inverse analysis.

Load-deflection ( $P$ - $\delta$ ) behaviors generated for two groups of HSFRC beams, tested under four-point flexural load, were used in NLFEA to back calculate the appropriate tensile  $\sigma$ - $\epsilon$  relationship of HSFRC beams. The first and second group of beams contains 65 kg/m<sup>3</sup> (0.76 %) of hook-end steel fibers and has concrete matrix strength of 70MPa and 90MPa, respectively. In the inverse analysis processes utilized here the tensile  $\sigma$ - $\epsilon$  relationship parameters are change, in the NLFEA model for beam-bending test, until experimental and numerically-determined  $P$ - $\delta$  behaviors reasonably match. The analyses indicated that the tensile  $\sigma$ - $\epsilon$  relationship of HSFRC can be successfully generated by inverse analysis utilizing experimentally measured  $P$ - $\delta$  behaviors of a beam.

## II. INVERSE ANALYSIS APPROACH

An inverse analysis, involving iterative procedure is used to derive the tensile  $\sigma$ - $\epsilon$  relationship from beam-bending test using the FEA package of ABAQUS<sup>®</sup>. The development of the tensile  $\sigma$ - $\epsilon$  relationship for specific HSFRC material includes. In the first step is to obtain a  $P$ - $\delta$  behavior from four-point bending beam test for the HSFRC under consideration. The second step involves the development finite element model to simulate the

H. A. Alguhi is a master student at King Saud University, Riyadh, KSA (phone: +966-538058320; fax: 303-555-5555; e-mail: halghui@ksu.edu.sa).

W. A. Elsaigh, is a PhD at King Saud University, Riyadh, KSA (phone: +966-11-4677032; e-mail: welsaigh@ksu.edu.sa).

beam bending test. In the third steps a first estimate of the tensile  $\sigma$ - $\varepsilon$  relationship is generated, using the RILEM TC 162-TDF and [3] models approaches, “for calculation (refer to the appendix)” to serve as an input with respect to the constitutive

relationship of the FEA. In the last step, the tensile  $\sigma$ - $\varepsilon$  relationship parameters are changed in the model until the experimental and numerically-determined P- $\delta$  behavior reach a reasonable match. Fig. 1 shows the inverse analysis process.

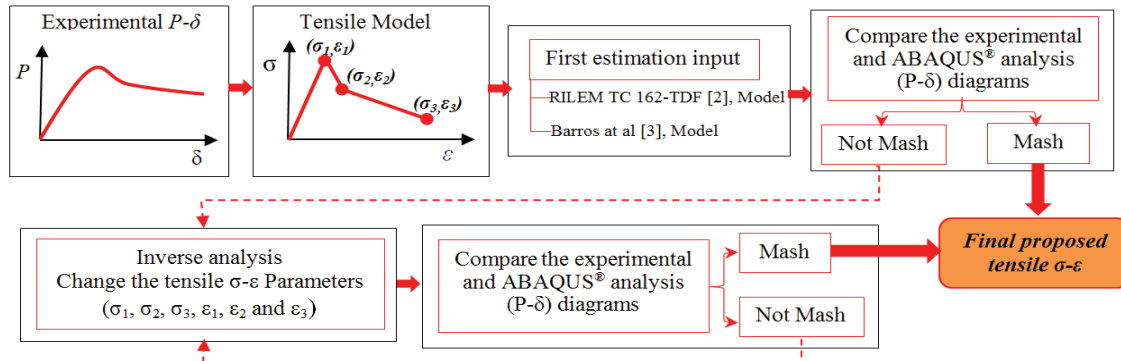


Fig. 1 Inverse analysis process

### III. FINITE ELEMENT MODEL

#### A. Mesh and Boundary Condition

A three-dimensional (3D) solid element of ABAQUS® named as “linear continuum three dimensional eight-node with reduced integration (C3D8R)” is chosen for intended. For this element, each node has three degrees of freedom (X, Y and Z), representing the displacements. The tested beam is measuring (600x150x150 mm) is divided into 861 elements with mesh size 25mm x 25mm x 25 mm. The same mesh was used and recommended for similar analysis conducted by [6], [7], [9]. Moreover, the mesh size affirmed by several ABAQUS® runs on the developed NLFE model to examine the mesh sensitivity. Static displacement-controlled load is used here without geometric non-linearity (NL-geom) formulation to simulate the experimental test setup as per ASTM C78-10. The boundary condition and mesh are shown in Fig. 2.

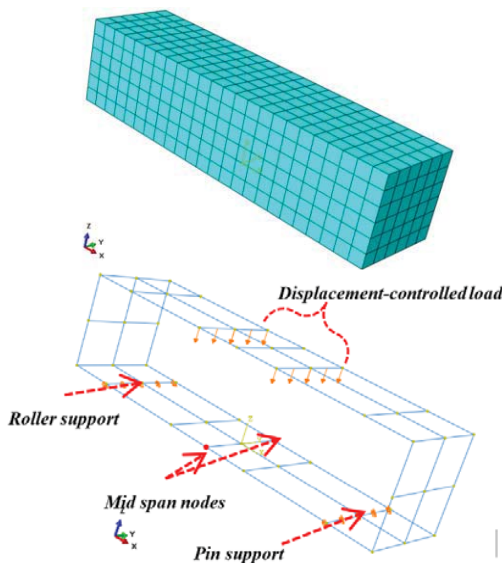


Fig. 2 Mesh and boundary conditions

#### B. Material Model

Concrete Damage Plasticity (CDP) formulations available in ABAQUS® are used in the current study. It is a continuum, plasticity-based model suitable for the analysis of concrete [7], [10]. Input concrete plasticity parameters including: dilation angle, potential eccentricity, and yield function factor are estimated as 37°, 0.1, and 0.67, respectively. The selected fall within the range of values reported in literature for similar analyses [9]–[12]. The well-known Drucker–Prager yield criterion is assumed for the analysis.

The first estimate of tensile  $\sigma$ - $\varepsilon$  relationship is determined, using the RILEM TC 162-TDF and [3] models for both tested concrete grade (70MPa and 90MPa). Moreover, the compressive  $\sigma$ - $\varepsilon$  relationship proposed by the RILEM TC 162-TDF model is adopted in the NLFEA for this study. Figs. 3 and 4 show the first estimate  $\sigma$ - $\varepsilon$  relationship (refer to the appendix for sample calculation).

Table I shows the average compressive strength and Young’s modulus measured using standard cylinder test according to ASTM C 39 2010 and ASTM C 469/C469M-10 2010 respectively. Typical Poisson’s ratio and concrete density are assumed for the proposed of this analysis.

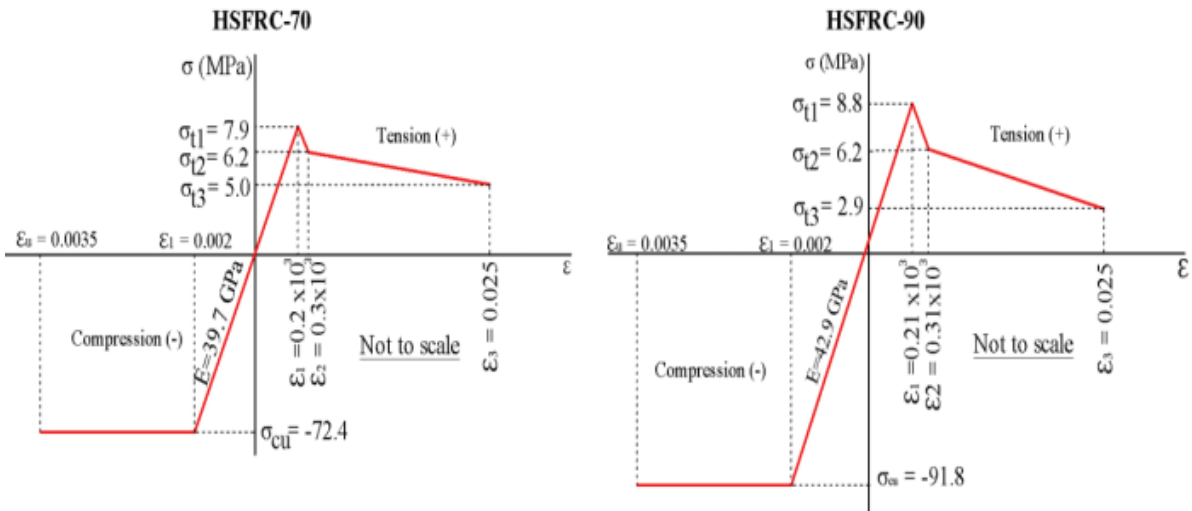
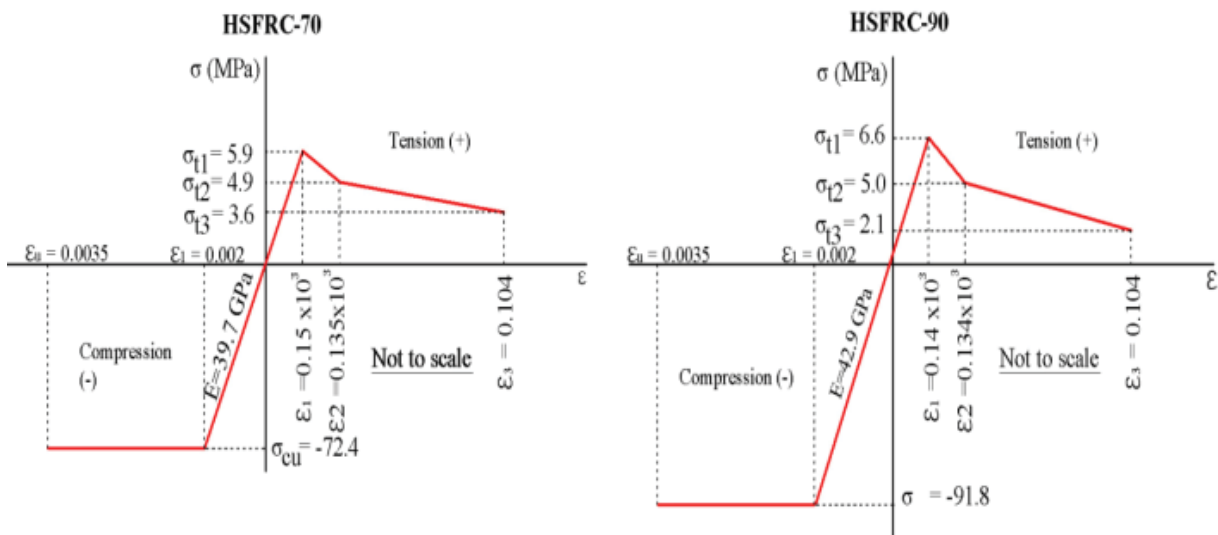
TABLE I  
A SUMMARY OF THE HSFRC PROPERTIES UTILIZED IN THE NLFEA

Beam	Cylinder strength (MPa)*	Young’s modulus (MPa)*	Poisson’s ratio**	Density (kg/mm <sup>3</sup> )**
HSFRC-70	72.4	34578	0.2	2.2 x 10 <sup>-9</sup>
HSFRC-90	91.8	39313		

(\*) Average of measured value,

(\*\*) Assumed value.

The Young’s modulus values used for the first estimation are those by the formula  $[E_C = 9500(f_{cm})^{1/3}]$  as given by the RILEM TC 162-TDF model as in Figs. 3 and 4. This is to evaluate the pertinence of HSFRC to the behavior given in this formula. This discrepancy between measured and calculated modulus is realized.


 Fig. 3 The first estimate of the  $\sigma$ - $\epsilon$  relationship for HSFRC according to RILEM, [2]

 Fig. 4 The first estimate of the  $\sigma$ - $\epsilon$  relationship for HSFRC according to [3]

#### IV. RESULTS AND DISCUSSION

Figs. 5 and 6 show the comparison between measured and numerically-calculated  $P$ - $\delta$  behavior for HSFRC-70 and HSFRC-90, respectively. The NLEEA using the estimate tensile  $\sigma$ - $\epsilon$  relationships reveal significant different in  $P$ - $\delta$  behavior. However, the first estimate calculated using [3] method seems to provide better estimation than RILEM method.

The first part of the  $P$ - $\delta$  curve has more slope than the measured curve. The slope of this part of the behavior is directly influence by the Young's modulus value. Therefore, the slope can be adjusted by reducing Young's modulus. It is obvious that the RILEM formula provides an overestimate for the modulus of HSFRC. This also confirmed by the measured Young's modulus presented in Table I.

The calculated flat part of  $P$ - $\delta$  curve (post the maximum load) is shifted up by a factor of approximately 1.5 as compared to the measured behavior. The tensile  $\sigma$ - $\epsilon$  relationship parameters that influence this part of the curve are discussed latter.

Fig. 7 shows the comparison between the proposed and the output compressive  $\sigma$ - $\epsilon$  responses. The output response is derived at integration point on the top part of the modeled beam. The comparison reveals that the actual maximum compressive stresses on the beam (12.7 MPa) are significantly less than compressive strength of HSFRC (72.4 and 91.8 MPa) considered here. Indeed, the failure of the HSFRC is mainly governed by cracking (tensile stress exceeds tensile strength). Therefore, assuming linear-elastic compressive  $\sigma$ - $\epsilon$  relation for the analysis of HSFRC beams would be satisfactory.

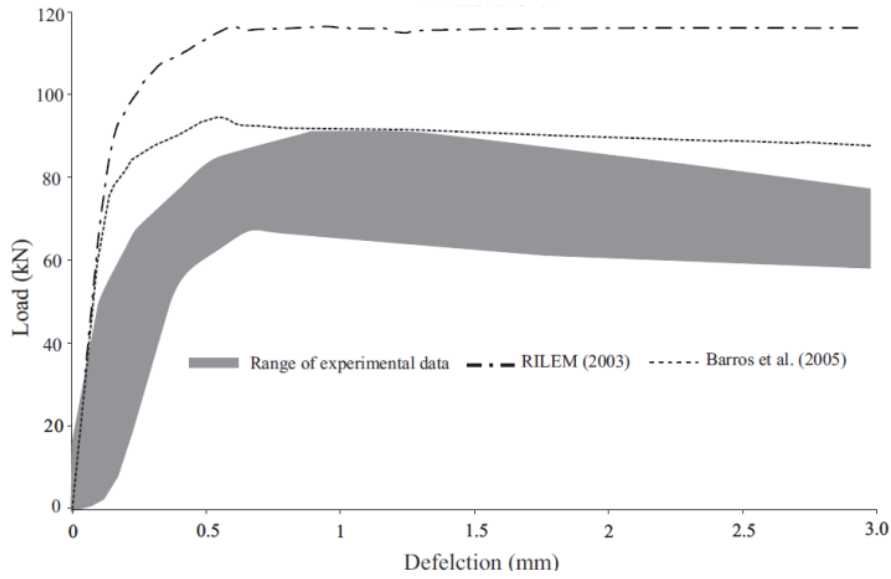


Fig. 5 Measured and calculated P- $\delta$  behaviors: First estimate  $\sigma$ - $\epsilon$  relationship-HSFRC-70

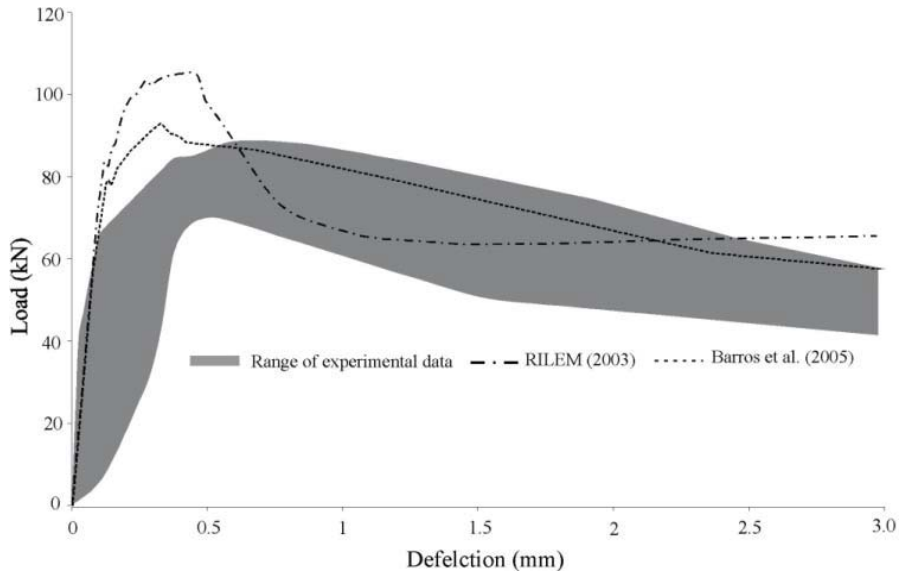


Fig. 6 Measured and calculated P- $\delta$  behaviors: First estimate  $\sigma$ - $\epsilon$  relationship-HSFRC-90

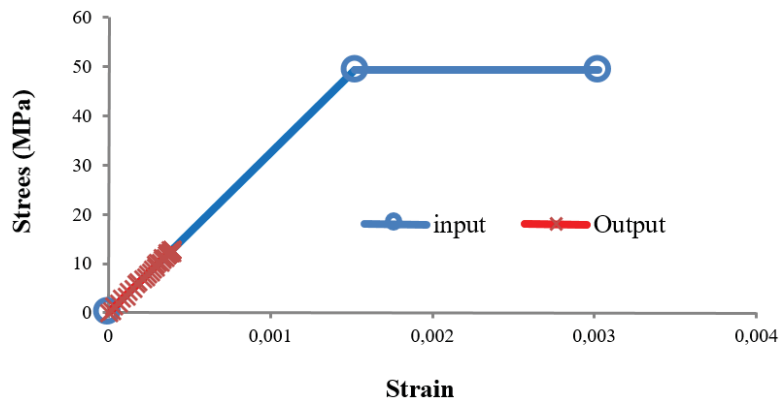


Fig. 7 Proposed input and output compressive  $\sigma$ - $\epsilon$  relationship

V. PROPOSED TENSILE STRESS-STRAIN RELATIONSHIP

The parameters of the first estimate tensile  $\sigma$ - $\epsilon$  relationship,  $\sigma_1, \sigma_2, \sigma_3, \epsilon_1, \epsilon_2$  and  $\epsilon_3$  (refer to Fig. 3) are systematically changed in the NLFE model until calculated and measured P- $\delta$  behaviors are matched.

The experience gained from the iterative analysis indicated that  $\sigma_1, \sigma_2, \sigma_3$  interrelated. In other words, their influence is not confined to particular part of the P- $\delta$  behavior. Changing the value of  $\sigma_1$  has considerable influence to the peak load but little effect on flat part of the P- $\delta$  behavior. The  $\sigma_2, \sigma_3$  remarkably affect the flat part with minimal influence on the peak load. The latter  $\sigma_3$  is more noticeable at higher deflection values on the P- $\delta$  behavior. The pre-peak part of the P- $\delta$  behavior is mainly influenced by the modulus value as discussed earlier.

Keeping in mind the narrow range of concrete strain values, the change in  $\epsilon_1, \epsilon_2$  and  $\epsilon_3$  is found to have insignificant influence on the P- $\delta$  behavior. Therefore, the strain values are kept unchanged during the analysis as per the RILEM model recommendation.

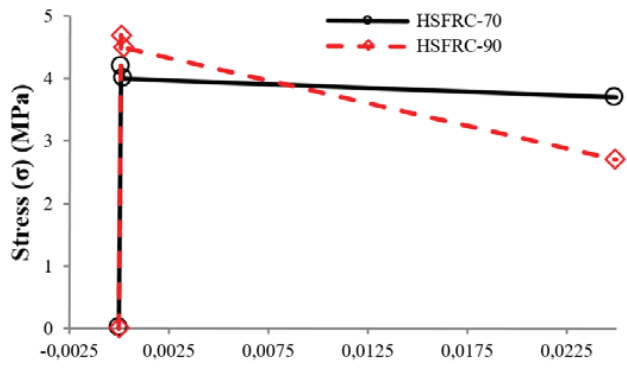
After several trials of change  $\sigma_1, \sigma_2$ , and  $\sigma_3$ , the calculated P- $\delta$  behavior reasonably matched the measured ones, as shown in Figs. 9 and 10. The slope on the pre-peak part of falls within the range of data but in the boarder of the steeper slope. The peak load and flat part of P- $\delta$  behavior fits reasonably. The tensile  $\sigma$ - $\epsilon$  relationships are given in Fig. 8.

VI. EFFECT OF MESH SIZE ON TENSILE  $\Sigma$ - $\epsilon$  RELATIONSHIP

In this section, the effect of mesh size on tensile  $\sigma$ - $\epsilon$  relationship is explored. For this propose the influence of four mesh sizes, 12.5mmx12.5mmx12.5mm, 25mmx25mmx25mm, 37.5mmx37.5mmx37.5mm and 75mmx75mmx75mm, on the 70 MPa beams were investigated. In the ABAQUS model, mesh size is changed while all other parameters are kept constant,

including the propose tensile  $\sigma$ - $\epsilon$  relationship shown in Fig. 9. The results of the analysis are shown in Fig. 11.

The results clearly indicate that the mesh size has an influence on the resulting P- $\delta$  behavior. The effect is more remarkable as the element size diverge from the original size (25mmx25mmx25mm) adopted initially while developing the tensile  $\sigma$ - $\epsilon$  relationship. This goes well with the concepts adapted by fracture mechanics, stating that material characteristics are element-size dependent [13]. In addition, element sizes grater /smaller than the original size profoundly influence the P- $\delta$  behavior beyond the cracking point.



B1-HSFRC-70		B2-HSFRC-90	
$\sigma$	$\epsilon$	$\sigma$	$\epsilon$
0.0	0.0	0.0	0.0
4.2	0.0001215	4.7	0.0001196
4.0	0.0002215	4.5	0.0002196
3.7	0.025	2.9	0.025

Fig. 8 Proposed tensile  $\sigma$ - $\epsilon$  relationships for HSFRC beams were adapted in NLFEA

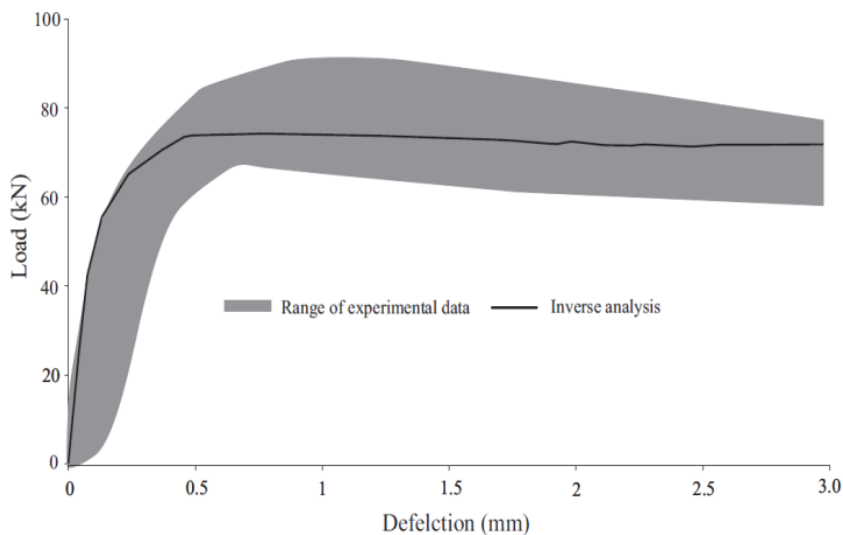


Fig. 9 Measured and calculated P- $\delta$  behaviors: Proposed  $\sigma$ - $\epsilon$  relationship-HSFRC-70

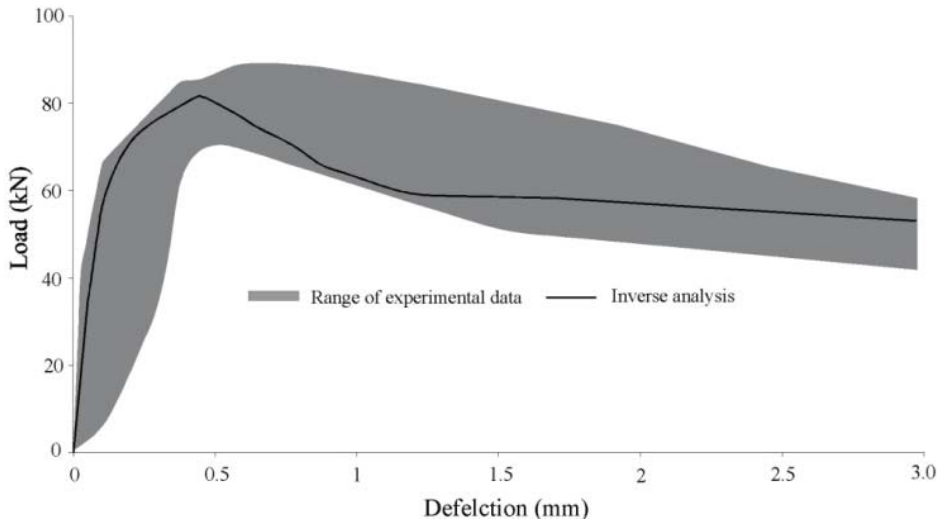


Fig. 10 Measured and calculated P-δ behaviors: Proposed  $\sigma$ - $\epsilon$  relationship-HSFRC-90

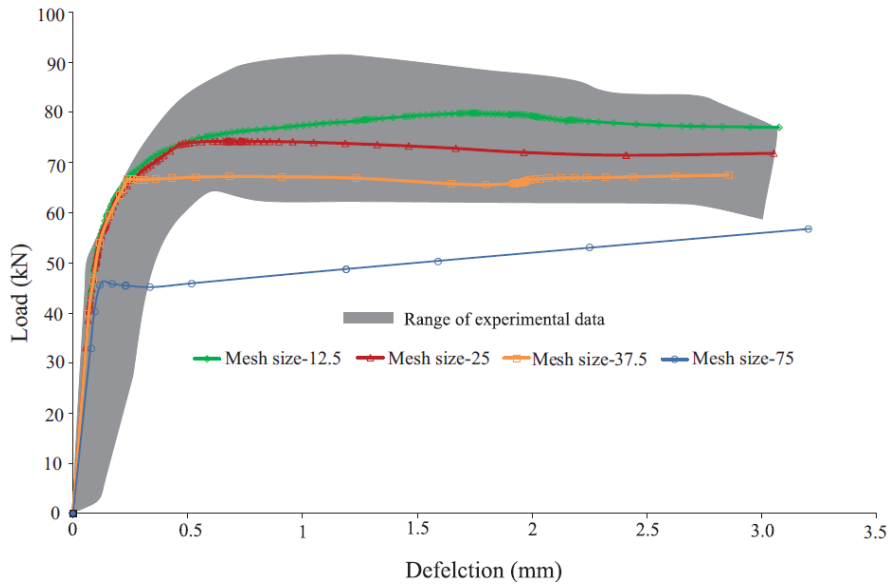


Fig. 11 Mesh sensitivity of HSFRC-70

VII. CONCLUSIONS

- 1- The RILEM and [3] methods are not suitable for estimating the tensile  $\sigma$ - $\epsilon$  relationship of HSFRC. However, the slope of the relationship to be appropriate.
- 2- The inverse analysis can be successfully used in ABAQUS® to appropriately determine the tensile  $\sigma$ - $\epsilon$  relationship of HSFRC, given that experimental data on P- $\delta$  behavior, compressive strength, and Young's modulus are available for the specific material.
- 3- The tensile  $\sigma$ - $\epsilon$  relationship is element-size dependent. In other words, different tensile  $\sigma$ - $\epsilon$  relationships are appropriate for different element-sizes. For NFELA incorporating HSFRC, the element size can be decided upon beforehand and the tensile  $\sigma$ - $\epsilon$  relationship can be generated accordingly.

- 4- The compressive  $\sigma$ - $\epsilon$  relationship can be satisfactory assumed to be linear for beam analysis.

APPENDIX

A. Tensile  $\sigma$ - $\epsilon$  Relationship of HSFRC-90 According the RILEM TC 162-TDF, [2]

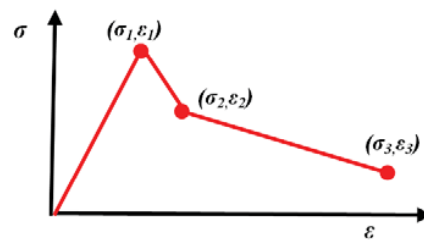


Fig. 12 The shape of tensile  $\sigma$ - $\epsilon$  relationship



1) Calculate the Proportionality Loads

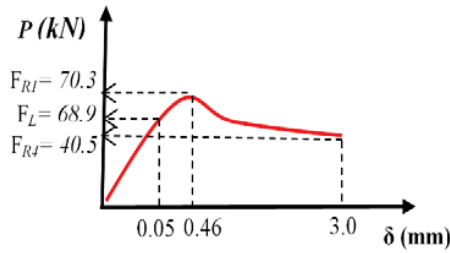


Fig. 13 Proportionality loads

2) Calculate Tensile Stress Values  $\sigma_1$ ,  $\sigma_2$ , and  $\sigma_3$

$$\text{Flexural strength} = \frac{3F_{R,i}L}{2bh_{sp}^2} \quad (1)$$

where  $b=150$  (width of beam),  $L=450$  (supported span),  $F_{R,i}=F_{R1}$  and  $F_{R4}$  as in Fig. 13,  $h_{sp}=150$  mm (effective depth of beam).

$$\sigma_{1 \text{ RILEM}} = f_{p1} * f_{ctm,fl} \left(1.6 - \frac{h_{sp}}{1000}\right) \quad (2)$$

$$\sigma_{2 \text{ RILEM}} = f_{p2} * f_{R,1} * k_h \quad (3)$$

$$\sigma_{3 \text{ RILEM}} = f_{p3} * f_{R,4} * k_h \quad (3)$$

where  $\sigma_i$  = stress (MPa),  $f_{Ri}$  = residual flexural tensile strength (MPa),  $h$  = height of the specimen (m),  $k_h$  = size factor,  $f_{ctm,fl}$  = flexural tensile strength (MP).  $f_p$  for  $\sigma_1$ ,  $\sigma_2$ , and  $\sigma_3$  = 0.7, 0.45 and 0.37 respectively.

$$k_h = 1 - 0.6 \frac{\left[\frac{h_{sp}}{10}\right] - 12.5}{47.5} \quad (5)$$

$$k_h = 1 - 0.6 \frac{\left[\frac{150}{10}\right] - 12.5}{47.5} \cong 0.97$$

$$\sigma_{1 \text{ RILEM}} = 0.7 * 8.7 \left(1.6 - \frac{150}{1000}\right) = 8.8 \text{ MPa}$$

$$\sigma_{2 \text{ RILEM}} = 0.45 * \left[\frac{3 * 70.3 * 10^3 * 450}{2 * 150^3}\right] * 0.97 = 6.2 \text{ MPa}$$

$$\sigma_{3 \text{ RILEM}} = 0.37 * \left[\frac{3 * 40.5 * 10^3 * 450}{2 * 150^3}\right] * 0.97 = 2.9 \text{ MPa}$$

3) Estimate the Young's Modulus  $E_c$

$$E_c = 9500(f_{cm})^{1/3}$$

where  $f_{cm} = 91.8$  MPa (mean compressive strength of HSFRC-90) (refer to Table I).

$$E_c = 9500 * (91.8)^{1/3} = 42855 \text{ MPa (42.9 GPa)}$$

4) Determine Tensile Strain Values  $\epsilon_1$ ,  $\epsilon_2$  and  $\epsilon_3$

$$\epsilon_1 = \sigma_1 / E_c = 8.8 / 42900 = 0.000184 \cong 0.21 \times 10^{-3}$$

$$\epsilon_2 = \epsilon_1 + 0.01\% = 0.2 \times 10^{-3} + 0.1 \times 10^{-3} = 0.31 \times 10^{-3}$$

$$\epsilon_3 = 2.5\% = 0.025$$

B. Tensile  $\sigma$ - $\epsilon$  Relationship of HSFRC-90 According to [3]

The model adapted the same shape of tensile  $\sigma$ - $\epsilon$  relationship, but modified the factor  $f_p$  in equations 2, 3 and 4. The adjusted  $f_p$  for  $\sigma_{1b}$ ,  $\sigma_{2b}$  and  $\sigma_{3b}$  are 0.52 and 0.27, respectively.

$$\sigma_{1b} = \sigma_1 * \frac{0.52}{0.7} = 6.5 \text{ MP}$$

$$\epsilon_1 = \sigma_1 / E_c = 6.5 / 42900 = 0.00015$$

$$\sigma_{2b} = \sigma_2 * \frac{0.36}{0.45} = 4.95 \cong 5 \text{ MPa}$$

$$\epsilon_2 = \epsilon_1 + 0.12\% = 0.15 \times 10^{-3} + 0.12 \times 10^{-2} = 0.135 \times 10^{-2}$$

$$\sigma_{2b} = \sigma_2 * \frac{0.27}{0.37} = 2.1 \text{ MPa}$$

$$\epsilon_3 = 10.4\% = 0.104$$

#### REFERENCES

- [1] Aldossari kMA. Behavior of High Strength Steel Fibers Reinforced Concrete Ground Slabs. Kingdom of Saudi Arabia: King Saud University, 2014.
- [2] Vandewalle L, Nemegeer D, Balazs L, Barr B, Barros J, Bartos P, et al. RILEM TC162-TDF: Test and Design Methods for Steel Fibre Reinforced Concrete: sigma-epsilon design method (final recommendation). Materials and Structures. 2003;36(262):560-7.
- [3] Barros JAO, Cunha VMCF, Ribeiro AF, Antunes JAB. Post-cracking behaviour of steel fibre reinforced concrete. Materials and Structures. 2005;38(1):47-56.
- [4] Kohoutkova, A., V. Kristek, and I. Broukalova, "Material model of FRC-inverse analysis" in Proc. 6th International RILEM Symposium, Italy, 2004, pp. 857-864.
- [5] Elsaigh W, Robberts J, Kearsley E, di Prisco M, Felicetti R, Plizzari G, "Modeling non-linear behavior of steel fibre reinforced concrete" in Proc. 6th International RILEM Symposium, Italy, 2004, pp. 837-846.
- [6] Tlemat H, Pilakoutas K, Neocleous K. Modelling of SFRC using inverse finite element analysis. Materials and Structures. 2006;39(2):221-33.
- [7] Labib WA. An experimental study and finite analysis of punching shear failure in steel fibre-reinforced concrete ground-suspended floor slabs: Liverpool John Moores University, 2008.
- [8] Hemmy O. Recommendations for finite element analysis of FRC-report of subtask 3.5. Brite-Euram project BRPR-CT98-0813: Test and Design Methods for Steel Fibre Reinforced Concrete, Project funded by the European Community under the Industrial and Materials Technologies Programme (Brite-Euram II), 2002.
- [9] Blazejowski M. Flexural Behaviour of Steel Fibre Reinforced Concrete Tunnel Linings. 2012.
- [10] Simulia D. ABAQUS 6.11 analysis user's manual. Abaqus. 2011;6:22.2.
- [11] Kmiecik P, Kamiński M. Modelling of reinforced concrete structures and composite structures with concrete strength degradation taken into consideration. Archives of Civil and Mechanical Engineering. 2011;11(3):623-36.
- [12] Jankowiak T, Lodygowski T. Identification of parameters of concrete damage plasticity constitutive model. 2013.
- [13] Anderson TL, Anderson T. Fracture mechanics: fundamentals and applications: CRC press, 2005.